

000 001 002 003 004 005 006 007 008 009 010 011 012 013 014 015 016 017 018 019 020 021 022 023 024 025 026 027 028 029 030 031 032 033 034 035 036 037 038 039 040 041 042 043 044 045 046 047 048 049 050 051 052 053 MALLVi: A MULTI-AGENT FRAMEWORK FOR INTE- GRATED GENERALIZED ROBOTICS MANIPULATION

Anonymous authors

Paper under double-blind review

ABSTRACT

Task-planning for robotic manipulation tasks using large language models (LLMs) is a relatively new phenomenon. Previous approaches have relied on training specialized models, fine-tuning pipeline components, or adapting LLMs with the setup through prompt tuning. However, many of these approaches lack environmental feedback. We introduce the MALLVi Framework, a **Multi-Agent Large Language and Vision** framework designed to solve robotic manipulation tasks that leverages closed-loop feedback from the environment. The agents are provided with an instruction in human language, along with an image of the current environment state. After thorough investigation and reasoning, MALLVi generates a series of realizable atomic instructions necessary for a supposed robot manipulator to complete the task. After extracting and executing low-level actions through the downstream agents, a Vision-Language Model (VLM) receives environmental feedback and prompts the framework either to repeat this procedure until success, or to proceed with the next atomic instruction. Our work shows that with careful prompt engineering, the integration of four LLM agents (**Decomposer**, **Localizer**, **Thinker**, and **Reflector**) can autonomously manage all compartments of a manipulation task - namely, initial perception, object localization, reasoning, and high-level planning. Moreover, the addition of a **Descriptor** agent can introduce a visual memory of the initial environment state in the pipeline. Crucially, compared to previous works, the reflecting agent can evaluate the completion or failure of each subtask. We validate our framework through experiments conducted both in simulated environments using VIMABench, RLBench and in real-world settings. Our framework handles diverse tasks, from standard manipulation benchmarks to custom user instructions. Our results show that the agents communicating to plan, execute, and evaluate the tasks iteratively not only lead to generalized performance but also increase average success rate in trials. The essential role of the reflecting in the pipeline is highlighted in experiments.

1 INTRODUCTION

Natural language tasks are rich, contextual, and often complicated —a simple sentence may be broken down to several smaller subtasks. With the advent of large language models (LLMs), attempts in the task-planning field for robotic manipulation have shifted to using complex language models. The question is clear: “How can we ground abstract instructions into robust, feedback-driven execution in dynamic environments?” As the scope of robotic applications expands, the core challenge has shifted: robots are no longer asked to repeat narrow, pre-programmed motions, but to understand flexible instructions and adapt to unpredictable situations. Existing methods have made progress on this front, typically following two strategies. The first learns behaviors directly from demonstrations, capturing motion trajectories with imitation or policy learning James et al. (2021); James & Davison (2021); Shridhar et al. (2022). The second relies on vision-language models (VLMs) to map natural language and visual input into actions Liu et al. (2024); Kim et al. (2024); Brohan et al. (2023; 2022). Both approaches have been effective in structured settings, but they falter when tasks involve open-vocabulary commands, new objects, or novel environments, where limited semantic understanding and adaptability restrict their use in real-world scenarios Zare et al. (2023); Sapkota et al. (2025).

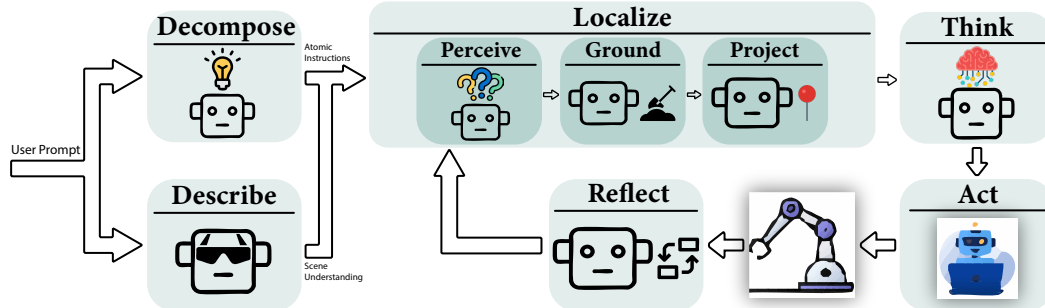
054 LLMs offer a promising path forward. They excel at reasoning and problem decomposition, and can
 055 translate high-level instructions into structured steps or even executable code Imani et al. (2023);
 056 Fang et al. (2024b). Frameworks that harness these capabilities demonstrate that LLMs can serve as
 057 powerful planners for robots Liang et al. (2022); Wang et al. (2024a); Fang et al. (2024a); Zawalski
 058 et al. (2024). However, these systems often operate in an open-loop manner: they generate plans
 059 once, without checking whether execution succeeds in practice. This makes them fragile in dynamic
 060 environments, where errors accumulate and hallucinations —plans that look valid in text but fail
 061 in the real world— can degrade performance Dhuliawala et al. (2023); Ali et al. (2024); Sun et al.
 062 (2024).

063 Recent research has taken steps toward closing the loop by integrating visual feedback for error
 064 detection and replanning Mei et al. (2024); Pchelintsev et al. (2025); Huang et al. (2022); Skreta
 065 et al. (2024); Huang et al. (2025). Yet, most of these systems rely on a single, monolithic model,
 066 which creates bottlenecks when tasks are ambiguous or when reasoning and perception need to be
 067 specialized. Moreover, relying on unconstrained LLMs/VLMs raises safety concerns, as unchecked
 068 outputs can lead to unsafe or adversarial behaviors Zhang et al. (2025).

069 In this paper, we introduce MALLVi (Fig. 1), a [multi-agent framework](#) for robotic task planning that
 070 directly addresses these challenges. Instead of relying on monolithic models, MALLVi coordinates
 071 specialized agents for perception, planning, and reflection, [enabling them to collaborate through a](#)
 072 [shared state](#). At its core, a decomposer agent translates human prompts into atomic instructions
 073 suitable for robotic execution. Subsequent agents handle environmental understanding, object local-
 074 ization, and trajectory planning through a low-level motion planner. A [reflector](#) agent continuously
 075 monitors the environment via visual feedback, [providing a closed-loop that identifies and reactivates](#)
 076 [only the specific failing agent for efficient error recovery](#). This distributed, feedback-driven de-
 077 sign enables MALLVi to disambiguate instructions, adapt to unexpected changes, and recover from
 078 errors—capabilities essential for real-world deployment.

079 Specifically, we:

- Propose MALLVi, a distributed framework [that introduces a genuine multi-agent architecture for robotics](#), combining LLM-based planning with VLM-based monitoring in a self-correcting process.
- Highlight the novel role of a [reflector](#) agent’s [targeted feedback loop](#), enabling reflection, error recovery, and adaptation through continuous environmental feedback.
- Validate MALLVi in both simulation (VIMABench Jiang et al. (2022), RLBench James et al. (2020)) and real-world experiments, demonstrating substantial improvements in success rate across diverse manipulation tasks [in a zero-shot setting](#).



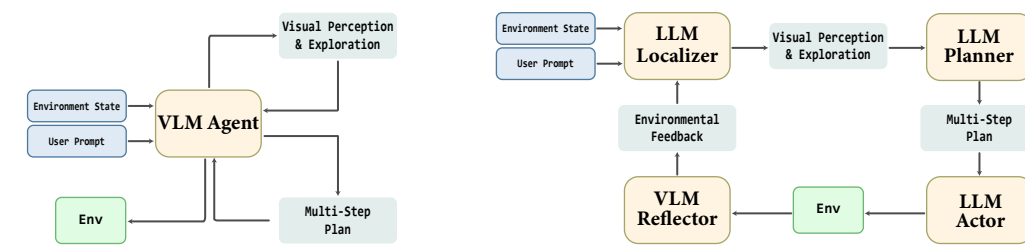
103 Figure 1: The MALLVi framework architecture. The pipeline processes user prompts through spe-
 104 cialized agents: **Decompose** breaks instructions into atomic steps, **Describe** provides scene un-
 105 derstanding, **Perceive** processes visual inputs, **Ground** localizes target objects, **Project** generates
 106 motion trajectories, **Think** coordinates high-level reasoning, **Act** executes robotic commands, and
 107 **Reflect** evaluates outcomes to enable iterative refinement and error recovery.

108
109
2 RELATED WORK110
111
2.1 LLMs AND VLMs FOR ROBOTIC TASK PLANNING112
113 The use of LLMs as high-level planners for robotics has grown rapidly in recent years. Frameworks
114 such as *Code-as-Policies* Liang et al. (2022) treat LLMs as translators that convert natural language
115 into parameterized API calls or executable code. *Inner Monologue* Huang et al. (2022) was an early
116 example of incorporating environmental feedback—including success and failure reports—to guide
117 the LLM’s planning. Subsequent work, such as LLM-Planner Song et al. (2023), demonstrated
118 few-shot planning for embodied agents by leveraging LLMs to generate sequences of pre-defined
119 actions. Similarly, *Tree-Planner* Hu et al. (2024) iteratively constructs a task tree using an LLM,
120 decomposing high-level goals into a sequence of executable subtasks.121 A central challenge in these approaches is the open-loop nature of the initial plans. To mitigate this,
122 recent research integrates visual feedback into replanning. For example, *Replan* Skreta et al. (2024)
123 combines an LLM for initial planning with a VLM to evaluate execution success, triggering replan-
124 ning upon failure. *ReplanVLM* Mei et al. (2024) and *LERa* Pchelintsev et al. (2025) similarly use
125 VLMs to detect visual errors and guide corrective action. *Look Before You Leap* Huang et al. (2025)
126 leverages GPT-4V to verify pre- and post-conditions for each planned step, while *CoPAL* Joublin
127 et al. (2024) introduces a self-corrective planning paradigm where the LLM critiques and refines its
128 own actions. Despite these advances, these systems are largely monolithic and limited in modularity,
129 often handling planning, perception, and execution in a tightly coupled manner. They typically lack
130 task-aware decomposition and flexible perception-action pipelines.131
132 2.2 MULTI-AGENT COLLABORATION AND REFLECTION133 The concept of using multiple LLM agents to collaborate, debate, or critique each other has proven
134 effective for complex problem-solving in non-embodied settings Sprigler et al. (2024); Wang et al.
135 (2024b). This idea is now being applied to robotics. *RoCo* Mandi et al. (2023) is a seminal work
136 that introduces dialectic collaboration between multiple LLM-controlled robots for task planning.137 Recent multi-agent approaches have further advanced collaboration in planning and manipulation.
138 *Wonderful Team* Wang et al. (2024c) presents a multi-agent VLLM framework where agents jointly
139 generate action sequences from a visual scene and task description, integrating perception and plan-
140 ning in an end-to-end system. *MALMM* Singh et al. (2024) employs three LLM agents (Planner,
141 Coder, Supervisor) to perform zero-shot block and object manipulation tasks, incorporating real-
142 time feedback and replanning to mitigate hallucinations and adapt to unseen tasks.143 Building on prior multi-agent LLM frameworks, our work adopts a modular multi-agent approach
144 for manipulation. Unlike previous methods, MALLVi tightly integrates perception, reasoning, and
145 execution in a collaborative agent pipeline, enabling robust adaptation and closed-loop correction in
146 complex environments.147
148 2.3 OPEN-VOCABULARY PERCEPTION149 Robust manipulation requires not just object localization, but context-aware grounding to resolve
150 ambiguities (e.g., “the red block” when there are multiple, referring to a past block). While foun-
151 dational models like OWL-ViT Minderer et al. (2022) and Grounding Dino Liu et al. (2023) pro-
152 vide open-vocabulary detection, they lack situational context. Segmentation models such as the
153 Segment Anything Model (SAM) Kirillov et al. (2023) offer general-purpose, high-quality seg-
154 mentation masks across diverse object categories. These capabilities make them well-suited for
155 downstream tasks such as grasp point extraction, where precise segmentation underpins reliable
156 interaction. However, they do not incorporate contextual reasoning or task grounding. Approaches
157 such as *SayCan* Ahn et al. (2022) address this gap by incorporating environmental cues, and recent
158 VLMs increasingly combine perception, grounding, and reasoning in a unified framework Bai et al.
159 (2023); Nasiriany et al. (2024). MALLVi builds on these advances by providing a modular, context-
160 aware perception pipeline that integrates detection, segmentation, and grounding to enable precise
161 manipulation.

162 3 METHODOLOGY

164 The MALLVi framework implements a multi-agent, self-correcting pipeline for robotic manipulation.
 165 Given a high-level user instruction and a real-time image of the environment, the system
 166 hierarchically decomposes tasks into atomic subtasks, grounds each to visual inputs, plans execu-
 167 tion trajectories, and adaptively refines actions based on feedback. Specialized agents communicate
 168 through object and memory tags, with automatic retry mechanism ensuring action success.

170 3.1 MULTI-AGENT



182 Figure 2: Comparison between single-agent and multi-agent frameworks.

185 Single-agent frameworks often struggle with maintaining task focus and performing sequential rea-
 186 soning in complex environments. As illustrated in Fig. 2, MALLVi mitigates these limitations by as-
 187 signing specialized agents to distinct execution aspects. This modular design reduces hallucinations,
 188 supports iterative refinement through closed-loop feedback, and improves overall task execution by
 189 maintaining focus and coherence.

190 3.1.1 DECOMPOSER-DESCRIPTOR AGENTS

192 The **Decomposer** and **Descriptor** agents operate in parallel at the first stage of the MALLVi pipeline,
 193 providing complementary functions for task execution.

194 The Decomposer agent converts a high-level instruction into a structured sequence of atomic sub-
 195 tasks. Each subtask corresponds to a primitive action in the Actor agent’s vocabulary (e.g., move,
 196 reach, push) and is annotated with memory tags containing parameters such as object identities,
 197 positions, or contextual references. Subtasks are executed sequentially, with a retry mechanism that
 198 allows failed steps to be reattempted without replanning the entire sequence. Implementation de-
 199 tails, including subtask representation, memory tagging, and fault-tolerant execution, are provided
 200 in Appendix section A.2, and A.3.

201 The Descriptor Agent generates a coarse representation of the environment using a vision-language
 202 model (VLM). It identifies objects, extracts the spatial relationships between them, and builds a spa-
 203 tial graph representing the scene. This graph enables the agent to reason about object configurations,
 204 constraints, and interactions, providing critical context for downstream perception, grounding, and
 205 planning agents.

206 By running in parallel, the Decomposer focuses on *what* needs to be done (task decomposition),
 207 while the Descriptor focuses on *where* and *how* in the environment (scene representation and rea-
 208 soning). Together, they align task objectives with environmental context from the outset.

210 3.1.2 LOCALIZER AGENT

- 212 • The **Perceptor** agent identifies task-relevant objects from the instruction and labels non-
 213 target objects. It refines grasping strategies (as explained in the Projector tool) across mul-
 214 tiple attempts, adapting to subtask failures and improving manipulation precision.
- 215 • The **Grounder** agent localizes objects in the image plane by integrating outputs from multi-
 216 ple detectors (GroundingDINO and OwlV2) to ensure reliable detection even under partial

216 failures. Beyond simple fusion, the agent employs a confidence-based selection mechanism: for each object, it weighs predictions from each detector according to model confidence and consistency with the spatial graph provided by the Descriptor agent. This allows
 217 the Grounder to provide accurate bounding boxes for downstream planning. By combining
 218 multi-model detection and confidence weighting, the Grounder agent ensures robust, high-
 219 fidelity localization essential for manipulation in dynamic and unstructured environments.
 220

- 221
- 222 • The **Projector** tool converts visual perception into actionable 3D grasp points, bridging the
 223 gap between scene understanding and robot execution.

224

225 **Grasp Point Extraction:** Leveraging the Segment Anything Model (SAM), the agent identifies
 226 candidate grasp points on objects. Object-specific heuristics are applied to select appropriate
 227 points (e.g., edges for cylindrical objects, centers for rigid blocks). A verification step ensures
 228 that each grasp point lies within the object’s segmentation mask, enhancing reliability and precision.

229

230 **3D Projection:** The extracted 2D grasp points are projected into 3D space using the depth
 231 map and the pinhole camera model. These 3D coordinates are subsequently converted
 232 into joint angles through inverse kinematics, producing executable targets for downstream
 233 planning and manipulation agents.

234 By integrating grasp point extraction and 3D projection within a single module, the Projector
 235 agent provides a direct and reliable interface between visual perception and robotic
 236 action. This design enables precise and consistent generation of executable 3D targets,
 237 supports closed-loop feedback during task execution, and preserves the modularity of the
 238 MALLVi framework, allowing seamless interaction with downstream planning and manipulation
 239 agents.

240

241 3.1.3 THINKER AGENT

242 The **Thinker** agent is an LLM responsible for translating high-level subtask information into action-
 243 able parameters for execution. It retrieves relevant objects (see section 3.1.1) and determines 3D
 244 grasp points along with any required rotations.

245 For tasks without prior memory (memoryless), the Thinker selects pick-and-place positions and rotations
 246 directly from the grasp points. For atomic instructions with associated memory tags, the
 247 agent identifies either source or target objects using the stored scene representation and spatial
 248 relationships, then computes corresponding pick-and-place positions and rotations based on the scene
 249 context.

251

252 3.1.4 ACTOR AGENT

253 The **Actor** agent executes the subtasks produced by the upstream agent. In both real-world deploy-
 254 ments and benchmark scenarios, the Actor interfaces with the environment through a predefined
 255 API, receiving the action parameters from the Thinker and performing the corresponding manipula-
 256 tion. This modular design allows the Actor to remain agnostic to high-level reasoning or low-level
 257 motion planning while ensuring accurate execution of planned actions.

258

259 3.1.5 REFLECTOR AGENT

260 The **Reflector** agent is a VLM responsible for verifying the execution of each subtask in real-time.
 261 After the Actor executes a subtask, the Reflector evaluates success using visual feedback. Suc-
 262 cessfully completed subtasks are removed from the execution queue, while failed subtasks trigger a
 263 reattempt from the beginning of the relevant subtask.

264 We demonstrate that the Reflector agent is essential for executing complex and sophisticated
 265 manipulation tasks, as evidenced by our ablation in Tables 1, 2, and 3. This iterative verification
 266 mechanism provides robust, closed-loop correction, ensuring that errors are detected and mitigated
 267 promptly. By continuously monitoring task execution, the Reflector agent enhances reliability and
 268 generalization across diverse and dynamic manipulation scenarios while preserving the modularity
 269 of the MALLVi framework.

270	High-Level	Demposer Agent “The main core”	High-Level	Descriptor Agent “Enabling memory utilization”
271	Responsibilities	<ul style="list-style-type: none"> Convert high-level instructions into atomic subtasks. Annotate subtasks parameters with tags (object, memory). Ensure sequential execution. 	Responsibilities	<ul style="list-style-type: none"> Build a coarse scene representation from visual input. Identify objects and their spatial relationships. Provide context for downstream planning.
272	Mid-Level	Localizer Agent “The computer vision toolkit”	Mid-Level	Thinker Agent “Compilation of compartments”
273	Responsibilities	<ul style="list-style-type: none"> Localize objects with confidence-based selection. Extract candidate source object and target object. Project 2D grasp points into 3D coordinates. 	Responsibilities	<ul style="list-style-type: none"> Compile state info into actionable 3D positions and rotations. Compute pick-and-place targets for the task. Retrieve objects from memory and scene representation.
274	Low-Level	Actor Agent “The doorway to environment”	Mid-Level	Reflector Agent “Closed-loop controller”
275	Responsibilities	<ul style="list-style-type: none"> Receive action parameters from Thinker agent. Execute subtasks through a predefined environment interface. Remain modular, independent of high-level reasoning. 	Responsibilities	<ul style="list-style-type: none"> Verify subtask execution in real-time. Remove completed subtasks or trigger reattempts on failure. Ensure closed-loop error correction for robust manipulation.
276				
277				
278				
279				
280				
281				
282				
283				
284				
285				
286				
287				
288				
289				

Figure 3: Analysis of specialized agents and their roles in a multi-agent system. Each agent functions at a designated level (high, mid, or low) to address specific components of task execution, including instruction decomposition, memory utilization, object localization, task reasoning, action execution, and closed-loop feedback provision.

4 EXPERIMENTS AND RESULTS

We evaluate MALLVi on both real-world manipulation tasks and benchmarked scenarios from VIMABench and RLBench. These tasks were selected for their alignment with real-world deployment settings, where the agent receives natural language instructions from users and perceives the environment solely through streaming camera input.

Real-world tasks: These are designed to reflect common robotic manipulation objectives:

- **Place Food** – tests accurate object placement.
- **Put Shape** – evaluates shape-specific placement.
- **Stack Blocks** – measures precision in stacking.
- **Shopping List** – requires sequential task execution.
- **Put in Mug** – tests fine-grained placement.
- **Math Ops** – evaluates math reasoning.
- **Stack Cups** – tests repetitive stacking skills.
- **Rearrange Objects** – requires organizing multiple objects according to instructions.

Examples of task stages are shown in Fig. 5.

VIMABench tasks: We selected a subset of VIMABench partitions with clear real-world analogues:

- **Simple Manipulation** – evaluates basic object handling.
- **Novel Concepts** – tests the agent’s ability to generalize to unseen object–instruction combinations.
- **Visual Reasoning** – requires reasoning under perceptual restrictions.
- **Visual Goal Reaching** – measures scene understanding and goal-directed planning.

RLBench tasks: These tasks require diverse skill sets in simulated environments:

Task Name	Prompt	Environment
Stack Blocks	Stack the blocks in red, green, blue order, bottom-up	
Sort Shape	Put the objects into the correct place	
Math Operation	Solve the mathematic equation	

Figure 4: Example of our real-world tasks. Stack Blocks, Sort Shape, and Math Operation each combine a specific prompt with a physical environment to assess an agent’s ability to act and solve problems in tangible settings.

- **Put in Safe** – tests accurate object placement under safety constraints.
- **Put in Drawer** – assesses sequential and goal-directed manipulation.
- **Stack Cups** – evaluates repetitive stacking.
- **Place Cups** – requires fine motor control in constrained settings.
- **Stack Blocks** – measures precision and planning in multi-step tasks.

4.1 REAL-WORLD TASKS

Real-world tasks capture conventional manipulation and reasoning skills. We reimplemented MALMM Singh et al. (2024) [VoxPoser](#) Huang et al. (2023), [ReKep](#) Huang et al. (2024) and used it as a baseline to evaluate our results in a real-world setting.

Method	Place Food	Put Shape	Stack Blocks	Shopping List	Put in Mug	Math Ops	Stack Cups	Rearrange Objects
MALMM	75	65	55	70	55	25	50	-
VoxPoser	70	55	40	45	40	15	35	0
ReKep	80	85	75	90	75	60	40	60
Single-Agent	25	10	15	10	30	5	10	0
w/o Reflector	85	60	60	65	55	70	50	45
MALLVi (Ours)	100	95	90	90	80	80	85	75

Table 1: Success rates (%) on 8 real-world tasks with 20 repetitions.

4.2 VIMABENCH TASKS

VIMABench tasks emphasize spatial reasoning, attribute binding, sequential planning, and state recall. VIMABench consists of 6 partitions and 17 tasks. We addressed 12 tasks in 4 partitions that were suitable for evaluating our pipeline. We compared our results against a prior work *Wonderful Team* Wang et al. (2024c), *CoTDiffusion* Ni et al. (2024a) and *PERIA* Ni et al. (2024b) which was also benchmarked using similar setup and tasks. For more details on our results for each task, refer to Table 6.

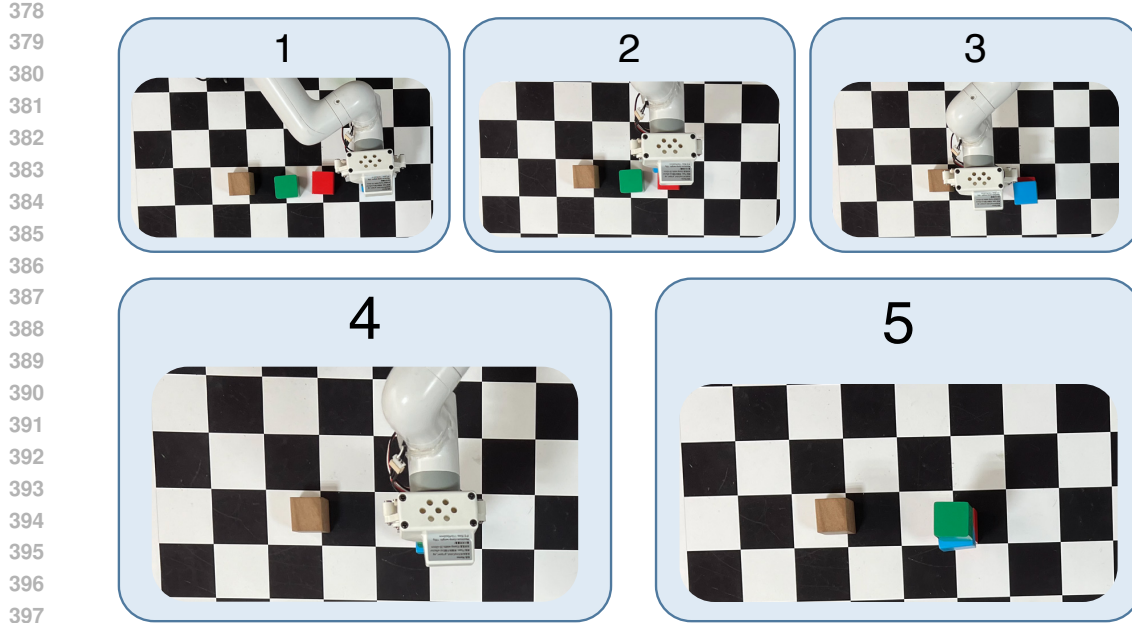


Figure 5: A real-world example of the **Stack Blocks** task. MALLVi is asked to stack the blocks in the order red, blue and green. The wooden block acts as a distraction.

Method	Simple Manipulation	Novel Concepts	Visual Reasoning	Visual Goal Reaching
Wonderful Team	100	85	90	-
CoDiffusion	86	70	54	44
PERIA	93	78	76	68
Single-Agent	25	10	15	10
w/o Reflector	100	80	30	40
MALLVi (Ours)	100	95	90	73

Table 2: Success rates (%) on VIMABench tasks on 100 repetitions.

4.3 RLBENCH TASKS

RLBench is another simulation platform that provides a large-scale benchmark for instruction-conditioned control. As a baseline for comparison, we use PerAct Shridhar et al. (2022) that has experimented using similar tasks.

Method	Put in Safe	Put in Drawer	Stack Cups	Place Cups	Stack Blocks
PerAct	44	68	0	0	36
Single-Agent	58	73	15	22	42
w/o Reflector	81	89	63	75	78
MALLVi (Ours)	92	94	83	96	90

Table 3: Success rates (%) on RLBench tasks with 100 repetition.

4.4 ABLATION STUDIES

To better understand the contribution of individual components, we conduct the following ablations:

4.4.1 SINGLE-AGENT BASELINE

We collapse all functionality into a single LLM agent, removing explicit task decomposition and modular specialization. Tables 1,2, and 3 compare this baseline with our multi-agent system. The results show that, while a single agent can handle simpler tasks, it struggles with compositional

432 reasoning and grounding. In contrast, the multi-agent system leverages specialized agents, leading
 433 to higher accuracy and greater robustness.
 434

435 **4.4.2 WITHOUT REFLECTOR**
 436

437 We remove the Reflector agent, eliminating the retry mechanism. Although subtasks are still exe-
 438 cuted in sequence, no verification step is performed. Tables 1, 2, and 3 compare the system with and
 439 without the Reflector. While the pipeline remains functional without it, verification and retry sig-
 440 nificantly improve reliability and overall task success rates. This is especially apparent for complex
 441 tasks, where potential for error is higher.
 442

443 **4.4.3 OPEN-SOURCE SUBSTITUTION**
 444

445 We replace GPT-4.1-mini (the default MALLVi backbone LLM) with open source models, including
 446 Qwen Qwen et al. (2025) + Qwen-VL Qwen et al. (2025) (3B and 7B) and LLaMA 3 Grattafiori
 447 et al. (2024) + LLaMA-Vision 3.2 (8B and 11B), to evaluate performance gaps between proprietary
 448 and publicly available systems. Table 4 summarizes the results. Although open source models
 449 perform competitively on simple tasks, they underperform on compositional and multimodal tasks.
 450 However, because MALLVi separates the task into several smaller duties for each agent, the pipeline
 451 still generally demonstrates acceptable accuracy relative to model size, indicating a core strength of
 452 our approach.
 453

Method	Simple Manipulation	Novel Concepts	Visual Reasoning	Visual Goal Reaching
GPT-4.1-MINI	100	95	95	73
QWEN-3B w/ QWEN-VL	70	54	10	46
QWEN-7B w/ QWEN-VL	85	50	30	62
LLAMA-3.1-8B w/ LLAMA-VISION-3.2-11B	80	50	27	59

454 **Table 4:** Success rates (%) on open-source models over 100 repetitions.
 455
 456
 457

461 **5 CONCLUSION**
 462

463 Our MALLVi framework leverages multiple LLM agents to plan and execute robotic manipulation
 464 tasks using closed-loop environmental feedback. Although this design enables robust high-level
 465 planning and iterative task refinement, it still relies on predefined atomic actions for execution,
 466 which constrains adaptability when the robot encounters unforeseen kinematic constraints, contact
 467 dynamics, or highly dynamic environments. This limitation reflects a broader trade-off between
 468 structured multi-agent reasoning and flexible low-level control.
 469

470 Future work should explore the integration of adaptive execution mechanisms, such as reinforcement
 471 learning or imitation learning controllers, or differentiable motion planning modules. Such exten-
 472 sions would allow atomic actions to be adapted at deployment time, complementing the iterative
 473 reasoning and reflection already provided by the agents. In addition, incorporating more sophisti-
 474 cated perception and grounding modules could improve performance in tasks with novel objects,
 475 complex textures, or highly dynamic scenes.
 476

477 MALLVi demonstrates that a multi-agent, closed-loop LLM framework can autonomously manage
 478 all key aspects of manipulation tasks, from perception and reasoning to high-level planning and
 479 reflection, leading to improved generalization and success rates. By combining structured reasoning
 480 with adaptive low-level execution, future iterations of MALLVi have the potential to achieve even
 481 greater robustness and autonomy in real-world robotic manipulation.
 482

483 **REFERENCES**
 484

485 Michael Ahn, Anthony Brohan, Noah Brown, Yevgen Chebotar, Omar Cortes, Byron David, Chelsea
 486 Finn, Keerthana Gopalakrishnan, Karol Hausman, Alexander Herzog, Daniel Ho, Jasmine Hsu,
 487 Julian Ibarz, Brian Ichter, Alex Irpan, Eric Jang, Rosario M Jauregui Ruano, Kyle Jeffrey, Sally
 488 Jesmonth, Nikhil Jayant Joshi, Ryan C. Julian, Dmitry Kalashnikov, Yuheng Kuang, Kuang-Huei
 489

- 486 Lee, Sergey Levine, Yao Lu, Linda Luu, Carolina Parada, Peter Pastor, Jornell Quiambao, Kan-
 487 ishka Rao, Jarek Rettinghouse, Diego M Reyes, Pierre Sermanet, Nicolas Sievers, Clayton Tan,
 488 Alexander Toshev, Vincent Vanhoucke, F. Xia, Ted Xiao, Peng Xu, Sichun Xu, and Mengyuan
 489 Yan. Do as i can, not as i say: Grounding language in robotic affordances. In *Conference on*
 490 *Robot Learning*, 2022.
- 491 Hassan Ali, Philipp Allgeuer, Carlo Mazzola, Giulia Belgiovine, Burak Can Kaplan, and Stefan
 492 Wermter. Robots can multitask too: Integrating a memory architecture and llms for enhanced
 493 cross-task robot action generation. *2024 IEEE-RAS 23rd International Conference on Humanoid*
 494 *Robots (Humanoids)*, pp. 811–818, 2024.
- 495 Jinze Bai, Shuai Bai, Shusheng Yang, Shijie Wang, Sinan Tan, Peng Wang, Junyang Lin, Chang
 496 Zhou, and Jingren Zhou. Qwen-vl: A versatile vision-language model for understanding, local-
 497 ization, text reading, and beyond. 2023.
- 498 Anthony Brohan, Noah Brown, Justice Carbajal, Yevgen Chebotar, Joseph Dabis, Chelsea Finn,
 499 Keerthana Gopalakrishnan, Karol Hausman, Alexander Herzog, Jasmine Hsu, Julian Ibarz, Brian
 500 Ichter, Alex Irpan, Tomas Jackson, Sally Jesmonth, Nikhil J. Joshi, Ryan C. Julian, Dmitry
 501 Kalashnikov, Yuheng Kuang, Isabel Leal, Kuang-Huei Lee, Sergey Levine, Yao Lu, Utsav Malla,
 502 Deeksha Manjunath, Igor Mordatch, Ofir Nachum, Carolina Parada, Jodilyn Peralta, Emily Perez,
 503 Karl Pertsch, Jornell Quiambao, Kanishka Rao, Michael S. Ryoo, Grecia Salazar, Pannag R. San-
 504 keti, Kevin Sayed, Jaspia Singh, Sumedh Anand Sontakke, Austin Stone, Clayton Tan, Huong
 505 Tran, Vincent Vanhoucke, Steve Vega, Quan Ho Vuong, F. Xia, Ted Xiao, Peng Xu, Sichun Xu,
 506 Tianhe Yu, and Brianna Zitkovich. Rt-1: Robotics transformer for real-world control at scale.
 507 *ArXiv*, abs/2212.06817, 2022.
- 508 Anthony Brohan, Noah Brown, Justice Carbajal, Yevgen Chebotar, Krzysztof Choromanski, Tianli
 509 Ding, Danny Driess, Kumar Avinava Dubey, Chelsea Finn, Peter R. Florence, Chuyuan Fu,
 510 Montse Gonzalez Arenas, Keerthana Gopalakrishnan, Kehang Han, Karol Hausman, Alexander
 511 Herzog, Jasmine Hsu, Brian Ichter, Alex Irpan, Nikhil J. Joshi, Ryan C. Julian, Dmitry Kalash-
 512 nikov, Yuheng Kuang, Isabel Leal, Sergey Levine, Henryk Michalewski, Igor Mordatch, Karl
 513 Pertsch, Kanishka Rao, Krista Reymann, Michael S. Ryoo, Grecia Salazar, Pannag R. Sanketi,
 514 Pierre Sermanet, Jaspia Singh, Anikait Singh, Radu Soricut, Huong Tran, Vincent Vanhoucke,
 515 Quan Ho Vuong, Ayzaan Wahid, Stefan Welker, Paul Wohlhart, Ted Xiao, Tianhe Yu, and Bri-
 516 anna Zitkovich. Rt-2: Vision-language-action models transfer web knowledge to robotic control.
 517 *ArXiv*, abs/2307.15818, 2023.
- 518 Shehzaad Dhuliawala, Mojtaba Komeili, Jing Xu, Roberta Raileanu, Xian Li, Asli Celikyilmaz,
 519 and Jason Weston. Chain-of-verification reduces hallucination in large language models. *ArXiv*,
 520 abs/2309.11495, 2023.
- 521 Kuan Fang, Fangchen Liu, Pieter Abbeel, and Sergey Levine. Moka: Open-world robotic manipu-
 522 lation through mark-based visual prompting. *Robotics: Science and Systems XX*, 2024a.
- 523 Meng Fang, Shilong Deng, Yudi Zhang, Zijing Shi, Ling Chen, Mykola Pechenizkiy, and Jun Wang.
 524 Large language models are neurosymbolic reasoners. *ArXiv*, abs/2401.09334, 2024b.
- 525 Aaron Grattafiori, Abhimanyu Dubey, Abhinav Jauhri, Abhinav Pandey, Abhishek Kadian, Ahmad
 526 Al-Dahle, Aiesha Letman, Akhil Mathur, Alan Schelten, Alex Vaughan, Amy Yang, Angela Fan,
 527 Anirudh Goyal, Anthony Hartshorn, Aobo Yang, Archi Mitra, Archie Sravankumar, Artem Ko-
 528 rennev, Arthur Hinsvark, Arun Rao, Aston Zhang, Aurelien Rodriguez, Austen Gregerson, Ava
 529 Spataru, Baptiste Roziere, Bethany Biron, Bin Tang, Bobbie Chern, Charlotte Caucheteux,
 530 Chaya Nayak, Chloe Bi, Chris Marra, Chris McConnell, Christian Keller, Christophe Touret,
 531 Chunyang Wu, Corinne Wong, Cristian Canton Ferrer, Cyrus Nikolaidis, Damien Allonsius,
 532 Daniel Song, Danielle Pintz, Danny Livshits, Danny Wyatt, David Esiobu, Dhruv Choudhary,
 533 Dhruv Mahajan, Diego Garcia-Olano, Diego Perino, Dieuwke Hupkes, Egor Lakomkin, Ehab
 534 AlBadawy, Elina Lobanova, Emily Dinan, Eric Michael Smith, Filip Radenovic, Francisco
 535 Guzmán, Frank Zhang, Gabriel Synnaeve, Gabrielle Lee, Georgia Lewis Anderson, Govind That-
 536 tai, Graeme Nail, Gregoire Mialon, Guan Pang, Guillem Cucurell, Hailey Nguyen, Hannah Kore-
 537 vaar, Hu Xu, Hugo Touvron, Iliyan Zarov, Imanol Arrieta Ibarra, Isabel Kloumann, Ishan Misra,
 538 Ivan Evtimov, Jack Zhang, Jade Copet, Jaewon Lee, Jan Geffert, Jana Vranes, Jason Park, Jay Ma-
 539 hadeokar, Jeet Shah, Jelmer van der Linde, Jennifer Billock, Jenny Hong, Janya Lee, Jeremy Fu,

540 Jianfeng Chi, Jianyu Huang, Jiawen Liu, Jie Wang, Jiecao Yu, Joanna Bitton, Joe Spisak, Jong-
 541 so Park, Joseph Rocca, Joshua Johnstun, Joshua Saxe, Junteng Jia, Kalyan Vasudevan Alwala,
 542 Karthik Prasad, Kartikeya Upasani, Kate Plawiak, Ke Li, Kenneth Heafield, Kevin Stone, Khalid
 543 El-Arini, Krithika Iyer, Kshitiz Malik, Kuenley Chiu, Kunal Bhalla, Kushal Lakhotia, Lauren
 544 Rantala-Yeary, Laurens van der Maaten, Lawrence Chen, Liang Tan, Liz Jenkins, Louis Martin,
 545 Lovish Madaan, Lubo Malo, Lukas Blecher, Lukas Landzaat, Luke de Oliveira, Madeline Muzzi,
 546 Mahesh Pasupuleti, Mannat Singh, Manohar Paluri, Marcin Kardas, Maria Tsimpoukelli, Mathew
 547 Oldham, Mathieu Rita, Maya Pavlova, Melanie Kambadur, Mike Lewis, Min Si, Mitesh Ku-
 548 mar Singh, Mona Hassan, Naman Goyal, Narjes Torabi, Nikolay Bashlykov, Nikolay Bogoy-
 549 chev, Niladri Chatterji, Ning Zhang, Olivier Duchenne, Onur Çelebi, Patrick Alrassy, Pengchuan
 550 Zhang, Pengwei Li, Petar Vasic, Peter Weng, Prajwal Bhargava, Pratik Dubal, Praveen Krishnan,
 551 Punit Singh Koura, Puxin Xu, Qing He, Qingxiao Dong, Ragavan Srinivasan, Raj Ganapathy, Ra-
 552 mon Calderer, Ricardo Silveira Cabral, Robert Stojnic, Roberta Raileanu, Rohan Maheswari, Ro-
 553 hit Girdhar, Rohit Patel, Romain Sauvestre, Ronnie Polidoro, Roshan Sumbaly, Ross Taylor, Ruan
 554 Silva, Rui Hou, Rui Wang, Saghar Hosseini, Sahana Chennabasappa, Sanjay Singh, Sean Bell,
 555 Seohyun Sonia Kim, Sergey Edunov, Shaoliang Nie, Sharan Narang, Sharath Raparth, Sheng
 556 Shen, Shengye Wan, Shruti Bhosale, Shun Zhang, Simon Vandenhende, Soumya Batra, Spencer
 557 Whitman, Sten Sootla, Stephane Collot, Suchin Gururangan, Sydney Borodinsky, Tamar Herman,
 558 Tara Fowler, Tarek Sheasha, Thomas Georgiou, Thomas Scialom, Tobias Speckbacher, Todor Mi-
 559 haylov, Tong Xiao, Ujjwal Karn, Vedanuj Goswami, Vibhor Gupta, Vignesh Ramanathan, Viktor
 560 Kerkez, Vincent Gonguet, Virginie Do, Vish Vogeti, Vitor Albiero, Vladan Petrovic, Weiwei
 561 Chu, Wenhan Xiong, Wenyin Fu, Whitney Meers, Xavier Martinet, Xiaodong Wang, Xiaofang
 562 Wang, Xiaoqing Ellen Tan, Xide Xia, Xinfeng Xie, Xuchao Jia, Xuewei Wang, Yaelle Gold-
 563 schlag, Yashesh Gaur, Yasmine Babaei, Yi Wen, Yiwen Song, Yuchen Zhang, Yue Li, Yuning
 564 Mao, Zacharie Delpierre Coudert, Zheng Yan, Zhengxing Chen, Zoe Papakipos, Aaditya Singh,
 565 Aayushi Srivastava, Abha Jain, Adam Kelsey, Adam Shajnfeld, Adithya Gangidi, Adolfo Victoria,
 566 Ahuva Goldstand, Ajay Menon, Ajay Sharma, Alex Boesenberg, Alexei Baevski, Allie Feinstein,
 567 Amanda Kallet, Amit Sangani, Amos Teo, Anam Yunus, Andrei Lupu, Andres Alvarado, An-
 568 drew Caples, Andrew Gu, Andrew Ho, Andrew Poulton, Andrew Ryan, Ankit Ramchandani, An-
 569 nie Dong, Annie Franco, Anuj Goyal, Aparajita Saraf, Arkabandhu Chowdhury, Ashley Gabriel,
 570 Ashwin Bharambe, Assaf Eisenman, Azadeh Yazdan, Beau James, Ben Maurer, Benjamin Leon-
 571 hardi, Bernie Huang, Beth Loyd, Beto De Paola, Bhargavi Paranjape, Bing Liu, Bo Wu, Boyu
 572 Ni, Braden Hancock, Bram Wasti, Brandon Spence, Brani Stojkovic, Brian Gamido, Britt Mon-
 573 talvo, Carl Parker, Carly Burton, Catalina Mejia, Ce Liu, Changhan Wang, Changkyu Kim, Chao
 574 Zhou, Chester Hu, Ching-Hsiang Chu, Chris Cai, Chris Tindal, Christoph Feichtenhofer, Cynthia
 575 Gao, Damon Civin, Dana Beaty, Daniel Kreymer, Daniel Li, David Adkins, David Xu, Davide
 576 Testuggine, Delia David, Devi Parikh, Diana Liskovich, Didem Foss, Dingkang Wang, Duc Le,
 577 Dustin Holland, Edward Dowling, Eissa Jamil, Elaine Montgomery, Eleonora Presani, Emily
 578 Hahn, Emily Wood, Eric-Tuan Le, Erik Brinkman, Esteban Arcaute, Evan Dunbar, Evan Smo-
 579 thers, Fei Sun, Felix Kreuk, Feng Tian, Filippos Kokkinos, Firat Ozgenel, Francesco Caggioni,
 580 Frank Kanayet, Frank Seide, Gabriela Medina Florez, Gabriella Schwarz, Gada Badeer, Georgia
 581 Swee, Gil Halpern, Grant Herman, Grigory Sizov, Guangyi, Zhang, Guna Lakshminarayanan,
 582 Hakan Inan, Hamid Shojaezeri, Han Zou, Hannah Wang, Hanwen Zha, Haroun Habeeb, Harri-
 583 son Rudolph, Helen Suk, Henry Aspegen, Hunter Goldman, Hongyuan Zhan, Ibrahim Damlaj,
 584 Igor Molybog, Igor Tufanov, Ilias Leontiadis, Irina-Elena Veliche, Itai Gat, Jake Weissman, James
 585 Geboski, James Kohli, Janice Lam, Japhet Asher, Jean-Baptiste Gaya, Jeff Marcus, Jeff Tang, Jen-
 586 nifer Chan, Jenny Zhen, Jeremy Reizenstein, Jeremy Teboul, Jessica Zhong, Jian Jin, Jingyi Yang,
 587 Joe Cummings, Jon Carvill, Jon Shepard, Jonathan McPhie, Jonathan Torres, Josh Ginsburg, Jun-
 588 jie Wang, Kai Wu, Kam Hou U, Karan Saxena, Kartikay Khandelwal, Katayoun Zand, Kathy
 589 Matosich, Kaushik Veeraraghavan, Kelly Michelena, Keqian Li, Kiran Jagadeesh, Kun Huang,
 590 Kunal Chawla, Kyle Huang, Lailin Chen, Lakshya Garg, Lavender A, Leandro Silva, Lee Bell,
 591 Lei Zhang, Liangpeng Guo, Licheng Yu, Liron Moshkovich, Luca Wehrstedt, Madian Khabsa,
 592 Manav Avalani, Manish Bhatt, Martynas Mankus, Matan Hasson, Matthew Lennie, Matthias
 593 Reso, Maxim Groshev, Maxim Naumov, Maya Lathi, Meghan Keneally, Miao Liu, Michael L.
 Seltzer, Michal Valko, Michelle Restrepo, Mihir Patel, Mik Vyatskov, Mikayel Samvelyan, Mike
 Clark, Mike Macey, Mike Wang, Miquel Jubert Hermoso, Mo Metanat, Mohammad Rastegari,
 Munish Bansal, Nandhini Santhanam, Natascha Parks, Natasha White, Navyata Bawa, Nayan
 Singhal, Nick Egebo, Nicolas Usunier, Nikhil Mehta, Nikolay Pavlovich Laptev, Ning Dong,
 Norman Cheng, Oleg Chernoguz, Olivia Hart, Omkar Salpekar, Ozlem Kalinli, Parkin Kent,

- 594 Parth Parekh, Paul Saab, Pavan Balaji, Pedro Rittner, Philip Bontrager, Pierre Roux, Piotr Dollar,
 595 Polina Zvyagina, Prashant Ratanchandani, Pritish Yuvraj, Qian Liang, Rachad Alao, Rachel Ro-
 596 driguez, Rafi Ayub, Raghatham Murthy, Raghu Nayani, Rahul Mitra, Rangaprabhu Parthasarathy,
 597 Raymond Li, Rebekkah Hogan, Robin Battey, Rocky Wang, Russ Howes, Ruty Rinott, Sachin
 598 Mehta, Sachin Siby, Sai Jayesh Bondu, Samyak Datta, Sara Chugh, Sara Hunt, Sargun Dhillon,
 599 Sasha Sidorov, Satadru Pan, Saurabh Mahajan, Saurabh Verma, Seiji Yamamoto, Sharadh Ra-
 600 maswamy, Shaun Lindsay, Shaun Lindsay, Sheng Feng, Shenghao Lin, Shengxin Cindy Zha,
 601 Shishir Patil, Shiva Shankar, Shuqiang Zhang, Shuqiang Zhang, Sinong Wang, Sneha Agarwal,
 602 Soji Sajuyigbe, Soumith Chintala, Stephanie Max, Stephen Chen, Steve Kehoe, Steve Satter-
 603 field, Sudarshan Govindaprasad, Sumit Gupta, Summer Deng, Sungmin Cho, Sunny Virk, Suraj
 604 Subramanian, Sy Choudhury, Sydney Goldman, Tal Remez, Tamar Glaser, Tamara Best, Thilo
 605 Koehler, Thomas Robinson, Tianhe Li, Tianjun Zhang, Tim Matthews, Timothy Chou, Tzook
 606 Shaked, Varun Vontimitta, Victoria Ajayi, Victoria Montanez, Vijai Mohan, Vinay Satish Ku-
 607 mar, Vishal Mangla, Vlad Ionescu, Vlad Poenaru, Vlad Tiberiu Mihailescu, Vladimir Ivanov,
 608 Wei Li, Wencheng Wang, Wenwen Jiang, Wes Bouaziz, Will Constable, Xiaocheng Tang, Xiao-
 609 jian Wu, Xiaolan Wang, Xilun Wu, Xinbo Gao, Yaniv Kleinman, Yanjun Chen, Ye Hu, Ye Jia,
 610 Ye Qi, Yenda Li, Yilin Zhang, Ying Zhang, Yossi Adi, Youngjin Nam, Yu, Wang, Yu Zhao,
 611 Yuchen Hao, Yundi Qian, Yunlu Li, Yuzi He, Zach Rait, Zachary DeVito, Zef Rosnbrick, Zhao-
 612 duo Wen, Zhenyu Yang, Zhiwei Zhao, and Zhiyu Ma. The llama 3 herd of models, 2024. URL
 613 <https://arxiv.org/abs/2407.21783>.
- 614 Andrew Hartley and Andrew Zisserman. Multiple view geometry in computer vision (2. ed.). 2006.
 615 URL <https://api.semanticscholar.org/CorpusID:8641226>.
- 616 Mengkang Hu, Yao Mu, Xinmiao Chelsey Yu, Mingyu Ding, Shiguang Wu, Wenqi Shao, Qiguang
 617 Chen, Bin Wang, Yu Qiao, and Ping Luo. Tree-planner: Efficient close-loop task planning with
 618 large language models. In *The Twelfth International Conference on Learning Representations*,
 619 2024. URL <https://openreview.net/forum?id=Glcso6z0e>.
- 620 Wenlong Huang, Fei Xia, Ted Xiao, Harris Chan, Jacky Liang, Pete Florence, Andy Zeng, Jonathan
 621 Tompson, Igor Mordatch, Yevgen Chebotar, Pierre Sermanet, Tomas Jackson, Noah Brown, Linda
 622 Luu, Sergey Levine, Karol Hausman, and brian ichter. Inner monologue: Embodied reasoning
 623 through planning with language models. In *6th Annual Conference on Robot Learning*, 2022.
 624 URL <https://openreview.net/forum?id=3R3Pz5i0tye>.
- 625 Wenlong Huang, Chen Wang, Ruohan Zhang, Yunzhu Li, Jiajun Wu, and Li Fei-Fei. Voxposer:
 626 Composable 3d value maps for robotic manipulation with language models. *arXiv preprint*
 627 *arXiv:2307.05973*, 2023.
- 628 Wenlong Huang, Chen Wang, Yunzhu Li, Ruohan Zhang, and Fei-Fei Li. Rekep: Spatio-temporal
 629 reasoning of relational keypoint constraints for robotic manipulation. *ArXiv*, abs/2409.01652,
 630 2024. URL <https://api.semanticscholar.org/CorpusID:272367253>.
- 631 Yuheng Huang, Jiayang Song, Zhijie Wang, Shengming Zhao, Huaming Chen, Felix Juefei-Xu, and
 632 Lei Ma. Look before you leap: An exploratory study of uncertainty analysis for large language
 633 models. *IEEE Transactions on Software Engineering*, 51(2):413–429, February 2025. ISSN
 634 2326-3881. doi: 10.1109/tse.2024.3519464. URL <http://dx.doi.org/10.1109/TSE.2024.3519464>.
- 635 Shima Imani, Liang Du, and H. Shrivastava. Mathprompter: Mathematical reasoning using large
 636 language models. In *Annual Meeting of the Association for Computational Linguistics*, 2023.
- 637 Stephen James and Andrew J. Davison. Q-attention: Enabling efficient learning for vision-based
 638 robotic manipulation. *IEEE Robotics and Automation Letters*, PP:1–1, 2021.
- 639 Stephen James, Zicong Ma, David Rovick Arrojo, and Andrew J. Davison. Rlbench: The robot
 640 learning benchmark & learning environment. *IEEE Robotics and Automation Letters*, 2020.
- 641 Stephen James, Kentaro Wada, Tristan Laidlow, and Andrew J. Davison. Coarse-to-fine q-attention:
 642 Efficient learning for visual robotic manipulation via discretisation. *2022 IEEE/CVF Conference*
 643 *on Computer Vision and Pattern Recognition (CVPR)*, pp. 13729–13738, 2021.

- 648 Yunfan Jiang, Agrim Gupta, Zichen Zhang, Guanzhi Wang, Yongqiang Dou, Yanjun Chen, Li Fei-
 649 Fei, Anima Anandkumar, Yuke Zhu, and Linxi (Jim) Fan. Vima: General robot manipulation with
 650 multimodal prompts. *ArXiv*, abs/2210.03094, 2022.
- 651
- 652 Frank Joublin, Antonello Ceravola, Pavel Smirnov, Felix Ocker, Joerg Deigmöller, Anna Belar-
 653 dinelli, Chao Wang, Stephan Hasler, Daniel Tanneberg, and Michael Gienger. Copal: Corrective
 654 planning of robot actions with large language models. In *2024 IEEE International Conference*
 655 *on Robotics and Automation (ICRA)*, pp. 8664–8670, 2024. doi: 10.1109/ICRA57147.2024.
 656 10610434.
- 657
- 658 Moo Jin Kim, Karl Pertsch, Siddharth Karamcheti, Ted Xiao, Ashwin Balakrishna, Suraj Nair,
 659 Rafael Rafailev, Ethan Foster, Grace Lam, Pannag R. Sanketi, Quan Vuong, Thomas Kollar,
 660 Benjamin Burchfiel, Russ Tedrake, Dorsa Sadigh, Sergey Levine, Percy Liang, and Chelsea Finn.
 661 Openvla: An open-source vision-language-action model. *ArXiv*, abs/2406.09246, 2024.
- 662
- 663 Alexander Kirillov, Eric Mintun, Nikhila Ravi, Hanzi Mao, Chloé Rolland, Laura Gustafson, Tete
 664 Xiao, Spencer Whitehead, Alexander C. Berg, Wan-Yen Lo, Piotr Dollár, and Ross B. Girshick.
 665 Segment anything. *2023 IEEE/CVF International Conference on Computer Vision (ICCV)*, pp.
 666 3992–4003, 2023.
- 667
- 668 Teyun Kwon, Norman Palo, and Edward Johns. Language models as zero-shot trajectory generators.
 669 *IEEE Robotics and Automation Letters*, PP:1–8, 07 2024. doi: 10.1109/LRA.2024.3410155.
- 670
- 671 Jacky Liang, Wenlong Huang, F. Xia, Peng Xu, Karol Hausman, Brian Ichter, Peter R. Florence,
 672 and Andy Zeng. Code as policies: Language model programs for embodied control. *2023 IEEE*
 673 *International Conference on Robotics and Automation (ICRA)*, pp. 9493–9500, 2022.
- 674
- 675 Jiaming Liu, Mengzhen Liu, Zhenyu Wang, Pengju An, Xiaoqi Li, Kaichen Zhou, Senqiao Yang,
 676 Renrui Zhang, Yandong Guo, and Shanghang Zhang. Robomamba: Efficient vision-language-
 677 action model for robotic reasoning and manipulation. In *Neural Information Processing Systems*,
 678 2024.
- 679
- 680 Shilong Liu, Zhaoyang Zeng, Tianhe Ren, Feng Li, Hao Zhang, Jie Yang, Chunyuan Li, Jianwei
 681 Yang, Hang Su, Jun Zhu, et al. Grounding dino: Marrying dino with grounded pre-training for
 682 open-set object detection. *arXiv preprint arXiv:2303.05499*, 2023.
- 683
- 684 Zhao Mandi, Shreeya Jain, and Shuran Song. Roco: Dialectic multi-robot collaboration with large
 685 language models. *2024 IEEE International Conference on Robotics and Automation (ICRA)*, pp.
 686 286–299, 2023.
- 687
- 688 Aoran Mei, Guo-Niu Zhu, Huaxiang Zhang, and Zhongxue Gan. Replanvlm: Replanning robotic
 689 tasks with visual language models. *IEEE Robotics and Automation Letters*, 9(11):10201–10208,
 690 2024. doi: 10.1109/LRA.2024.3471457.
- 691
- 692 Matthias Minderer, Alexey A. Gritsenko, Austin Stone, Maxim Neumann, Dirk Weissenborn,
 693 Alexey Dosovitskiy, Aravindh Mahendran, Anurag Arnab, Mostafa Dehghani, Zhuoran Shen,
 694 Xiao Wang, Xiaohua Zhai, Thomas Kipf, and Neil Houlsby. Simple open-vocabulary object
 695 detection with vision transformers. *ArXiv*, abs/2205.06230, 2022.
- 696
- 697 Soroush Nasiriany, Fei Xia, Wenhao Yu, Ted Xiao, Jacky Liang, Ishita Dasgupta, Annie Xie, Danny
 698 Driess, Ayzaan Wahid, Zhuo Xu, Quan Ho Vuong, Tingnan Zhang, Tsang-Wei Edward Lee,
 699 Kuang-Huei Lee, Peng Xu, Sean Kirmani, Yuke Zhu, Andy Zeng, Karol Hausman, Nicolas Man-
 700 fred Otto Heess, Chelsea Finn, Sergey Levine, and Brian Ichter. Pivot: Iterative visual prompting
 701 elicits actionable knowledge for vlms. *ArXiv*, abs/2402.07872, 2024.
- 702
- 703 Fei Ni, Jianye Hao, Shiguang Wu, Longxin Kou, Jiashun Liu, Yan Zheng, Bin Wang, and Yuzheng
 704 Zhuang. Generate subgoal images before act: Unlocking the chain-of-thought reasoning in
 705 diffusion model for robot manipulation with multimodal prompts. In *2024 IEEE/CVF Con-
 706 ference on Computer Vision and Pattern Recognition (CVPR)*, pp. 13991–14000, 2024a. doi:
 707 10.1109/CVPR52733.2024.01327.

- 702 Fei Ni, Jianye Hao, Shiguang Wu, Longxin Kou, Yifu Yuan, Zibin Dong, Jinyi Liu, Mingzhi
 703 Li, Yuzheng Zhuang, and Yan Zheng. Peria: Perceive, reason, imagine, act via holistic
 704 language and vision planning for manipulation. In A. Globerson, L. Mackey, D. Belgrave,
 705 A. Fan, U. Paquet, J. Tomczak, and C. Zhang (eds.), *Advances in Neural Information Processing
 706 Systems*, volume 37, pp. 17541–17571. Curran Associates, Inc., 2024b. doi: 10.52202/
 707 079017-0558. URL https://proceedings.neurips.cc/paper_files/paper/2024/file/1f6af963e891e7efa229c24a1607fa7f-Paper-Conference.pdf.
- 709 Svyatoslav Pchelintsev, Maxim Patratskiy, Anatoly Onishchenko, Aleksandr Korchemnyi, Aleksandr
 710 Medvedev, Uliana Vinogradova, Ilya Galuzinsky, Aleksey Postnikov, Alexey K. Kovalev, and
 711 Aleksandr I. Panov. Lera: Replanning with visual feedback in instruction following, 2025. URL
 712 <https://arxiv.org/abs/2507.05135>.
- 713 Qwen, :, An Yang, Baosong Yang, Beichen Zhang, Binyuan Hui, Bo Zheng, Bowen Yu, Chengyuan
 714 Li, Dayiheng Liu, Fei Huang, Haoran Wei, Huan Lin, Jian Yang, Jianhong Tu, Jianwei Zhang,
 715 Jianxin Yang, Jiaxi Yang, Jingren Zhou, Junyang Lin, Kai Dang, Keming Lu, Keqin Bao, Kexin
 716 Yang, Le Yu, Mei Li, Mingfeng Xue, Pei Zhang, Qin Zhu, Rui Men, Runji Lin, Tianhao Li,
 717 Tianyi Tang, Tingyu Xia, Xingzhang Ren, Xuancheng Ren, Yang Fan, Yang Su, Yichang Zhang,
 718 Yu Wan, Yuqiong Liu, Zeyu Cui, Zhenru Zhang, and Zihan Qiu. Qwen2.5 technical report, 2025.
 719 URL <https://arxiv.org/abs/2412.15115>.
- 720 Ranjan Sapkota, Yang Cao, Konstantinos I. Roumeliotis, and Manoj Karkee. Vision-language-action
 721 models: Concepts, progress, applications and challenges. 2025.
- 723 Mohit Shridhar, Lucas Manuelli, and Dieter Fox. Perceiver-actor: A multi-task transformer for
 724 robotic manipulation. *ArXiv*, abs/2209.05451, 2022.
- 725 Harsh Singh, Rocktim Jyoti Das, Mingfei Han, Preslav Nakov, and Ivan Laptev. Malmm: Multi-
 726 agent large language models for zero-shot robotics manipulation. *ArXiv*, abs/2411.17636, 2024.
- 728 Marta Skreta, Zihan Zhou, Jia Lin Yuan, Kourosh Darvish, Alan Aspuru-Guzik, and Animesh Garg.
 729 RePLan: Robotic replanning with perception and language models, 2024. URL <https://openreview.net/forum?id=gisAooH2TG>.
- 731 Chan Hee Song, Jiaman Wu, Clayton Washington, Brian M. Sadler, Wei-Lun Chao, and Yu Su.
 732 Llm-planner: Few-shot grounded planning for embodied agents with large language models. In
 733 *Proceedings of the IEEE/CVF International Conference on Computer Vision (ICCV)*, October
 734 2023.
- 735 Asher Sprigler, Alexander Drobek, Keagan Weinstock, Wendpanga Tapsoba, Gavin Childress, Andy
 736 Dao, and Lucas Gral. Synergistic simulations: Multi-agent problem solving with large language
 737 models, 2024. URL <https://arxiv.org/abs/2409.13753>.
- 739 Wenhao Sun, Sai Hou, Zixuan Wang, Bo Yu, Shaoshan Liu, Xu Yang, Shuai Liang, Yiming Gan, and
 740 Yinhe Han. Dadu-e: Rethinking the role of large language model in robotic computing pipeline.
 741 *ArXiv*, abs/2412.01663, 2024.
- 742 Jiaqi Wang, Zihao Wu, Yiwei Li, Hanqi Jiang, Peng Shu, Enze Shi, Huawei Hu, Chong-Yi Ma,
 743 Yi-Hsueh Liu, Xuhui Wang, Yincheng Yao, Xuan Liu, Huaqin Zhao, Zheng Liu, Haixing Dai,
 744 Lin Zhao, Bao Ge, Xiang Li, Tianming Liu, and Shu Zhang. Large language models for robotics:
 745 Opportunities, challenges, and perspectives. *ArXiv*, abs/2401.04334, 2024a.
- 747 Noah Wang, Z.y. Peng, Haoran Que, Jiaheng Liu, Wangchunshu Zhou, Yuhang Wu, Hongcheng
 748 Guo, Ruitong Gan, Zehao Ni, Jian Yang, Man Zhang, Zhaoxiang Zhang, Wanli Ouyang, Ke Xu,
 749 Wenhao Huang, Jie Fu, and Junran Peng. RoleLLM: Benchmarking, eliciting, and enhancing role-
 750 playing abilities of large language models. In Lun-Wei Ku, Andre Martins, and Vivek Srikumar
 751 (eds.), *Findings of the Association for Computational Linguistics: ACL 2024*, pp. 14743–14777,
 752 Bangkok, Thailand, August 2024b. Association for Computational Linguistics. doi: 10.18653/
 753 v1/2024.findings-acl.878. URL <https://aclanthology.org/2024.findings-acl.878/>.
- 755 Zidan Wang, Rui Shen, and Bradly C. Stadie. Wonderful team: Zero-shot physical task planning
 with visual llms. 2024c.

756 Maryam Zare, Parham Mohsenzadeh Kebria, Abbas Khosravi, and Saeid Nahavandi. A survey
 757 of imitation learning: Algorithms, recent developments, and challenges. *IEEE Transactions on*
 758 *Cybernetics*, 54:7173–7186, 2023.

760 Michal Zawalski, William Chen, Karl Pertsch, Oier Mees, Chelsea Finn, and Sergey Levine. Robotic
 761 control via embodied chain-of-thought reasoning. In *Conference on Robot Learning*, 2024.

762 Hangtao Zhang, Chenyu Zhu, Xianlong Wang, Ziqi Zhou, Changgan Yin, Minghui Li, Lulu Xue,
 763 Yichen Wang, Shengshan Hu, Aishan Liu, Peijin Guo, and Leo Yu Zhang. Badrobot: Jailbreaking
 764 embodied LLMs in the physical world. In *The Thirteenth International Conference on Learning*
 765 *Representations*, 2025. URL <https://openreview.net/forum?id=ei3qCntB66>.

767 A APPENDIX

770 A.1 AGENTS

771 Each agent serves a critical function in the end-to-end execution pipeline for user instructions. We
 772 demonstrate why each component is indispensable, accompanied by explaining its functionality in
 773 detail.

775 Our stack uses LangGraph¹, enabling easy integration and changes, rendering ablation studies
 776 much simpler. A custom LangGraph wrapper with proper logging (for debugging purposes) was
 777 implemented. A log visualizer utilizing Dash² serves as the primary debugging tool to visualize
 778 inter-agent interactions over time, using the log outputs from the LangGraph wrapper.

780 Listing 1: GraphState Class

```

781 1 class GraphState:
782 2
783 3     taskname: str
784 4     original_prompt: str
785 5     initial_decomposition_done: bool
786 6     decomposed_prompts: list[str]
787 7     queue: list[str]
788 8     current_prompt: str
789 9     should_terminate: bool
790 10    multi_object: bool
791 11
792 12
793 13    object_of_interest: str
794 14    not_object_of_interest: str
795 15    all_objects: list[str]
796 16    results: dict[str, dict]
797 17
798 18
799 19    image: Image
800 20    depth_image: Matrix
801 21    camera_matrix: 3x3 Matrix
802 22    rotation_matrix: 3x3 Matrix
803 23    translation_vector: 3x1 Matrix
804 24
805 25
806 26    grounder_output: list[Detection]
807 27    grasp_points: list[GraspPoint2D]
808 28    grasp_points_3d: list[GraspPoint3D]
809 29    thinker_output: dict[str, ThinkerOutput]
810 30    actor_output: dict[str, ActorOutput]
811 31    reflection_output: dict[str, ReflectionResult]
812 32

```

¹link

²link

```

810
811     scene_description: Graph
812     detected_objects: list[dict]
813     descriptor_grasp_points: list[GraspPoint2D]
814     descriptor_grasp_points_3d: list[GraspPoint3D]
815
816
817

```

Listing 2: MultiAgentRoboticSystem Class

```

818 class MultiAgentRoboticSystem:
819
820     def initialize_system(self) -> GraphState:
821         state = GraphState()
822         state.should_terminate = False
823         state.initial_decomposition_done = False
824         state.queue = []
825         state.results = {}
826         return state
827
828     def run_main_pipeline(self, state: GraphState) -> GraphState:
829         if not state.initial_decomposition_done:
830             state = decomposer_node(state)
831             state.initial_decomposition_done = True
832
833         descriptor_result = descriptor_node(state)
834
835         while state.queue and not state.should_terminate:
836             state.current_prompt = state.queue.pop(0)
837
838             perception_result = perceptor_node(state)
839
840             grounding_result = grounder_node(state)
841
842             segmentation_result = segmentor_node(state)
843
844             projection_result = projector_node(state)
845
846             planning_result = thinker_node(state)
847
848             execution_result = actor_node(state)
849
850             reflection_result = reflector_node(state)
851
852             state.results[state.current_prompt] = {
853                 'thinker_output': state.thinker_output[state.
854                     current_prompt],
855                 'actor_output': state.actor_output[state.
856                     current_prompt],
857                 'reflection_output': state.reflection_output[state.
858                     current_prompt]
859             }
860
861         return state
862
863

```

A.2 DECOMPOSER AS THE MAIN CORE

The Decomposer agent is responsible for converting high-level instructions into structured, executable sequences of subtasks, providing the critical interface between abstract task specifications and the Actor agent’s primitive actions. This appendix details the internal mechanisms, representation, and execution logic of the Decomposer.

864 SUBTASK GENERATION

865

866 Upon receiving a high-level instruction, the Decomposer generates a hierarchical sequence of sub-
 867 tasks. Each subtask corresponds to a primitive action in the Actor agent's vocabulary, such as:

868

- 869 • move — navigating to a target location.
- 870 • reach — extending an agent manipulator toward an object.
- 871 • push — applying force to move an object.

872

873 Each subtask represents an atomic unit of work that can be executed independently while preserving
 874 the logical structure of the overall task.

875

876 MEMORY TAGGING AND PARAMETERIZATION

877

878 Subtasks are annotated with memory tags that provide all necessary execution parameters. These
 879 tags may include:

880

- 881 • Object identifiers and properties (e.g., size, type, affordances).
- 882 • Spatial positions and orientations.
- 883 • Contextual references derived from the environment or previous subtasks.

884

885 Memory tags enable the Actor agent to resolve ambiguities, maintain task consistency, and adapt
 886 dynamically if the environment changes during execution.

887

This agent's instruction prompt is shown in Fig. 8, and 9

888

889 A.3 DESCRIPTOR, ENABLING MEMORY UTILIZATION

890

891 VISION-LANGUAGE MODEL (VLM) INTEGRATION

892

893 The Descriptor leverages a pre-trained vision-language model to interpret raw sensory input and
 894 extract semantically meaningful information. Specifically, it:

895

- 896 • Detects and classifies objects in the environment.
- 897 • Generates descriptive embeddings that capture object properties (e.g., type, color, size,
 affordances).
- 898 • Associates textual and visual modalities, enabling grounding of high-level instructions to
 perceptual features.

899

900 SPATIAL RELATIONSHIP EXTRACTION

901

902 Beyond individual object recognition, the Descriptor agent computes pairwise spatial relationships
 903 to capture the scene configuration. For each object pair, it encodes relationships such as:

904

- 905 • Relative positions (e.g., left, right, above, below).
- 906 • Distances and proximities.
- 907 • Interaction constraints (e.g., support, containment, adjacency).

908

909 These relational encodings are essential for reasoning about feasible actions, dependencies, and
 910 constraints in the environment.

911

912 GRAPH-BASED SCENE REPRESENTATION

913

914 The agent constructs a spatial graph where nodes correspond to detected objects and edges encode
 915 the extracted spatial relationships. This graph structure provides:

916

- 917 • A structured memory format for storing object and relational information.

- 918 • An interface for downstream agents to query object configurations, constraints, and potential
 919 interactions.
 920
 921 • Support for reasoning over both local neighborhoods (adjacent objects) and global scene
 922 layout.

923 **MEMORY UTILIZATION AND AGENT INTERACTION**

925 The spatial graph generated by the Descriptor agent is stored in a memory-accessible format, en-
 926 abling other agents to:

- 928 • Query the environment efficiently without repeated perception.
 929 • Ground high-level instructions in the observed scene.
 930
 931 • Plan and decompose tasks based on the current state and object interactions.

933 By serving as a centralized, structured memory representation, the Descriptor facilitates coordina-
 934 tion among perception, planning, and execution agents. This agent's prompt is shown in Fig. 10

936 **A.4 THINKER COMPILEMENT OF COMPARTMENTS**

938 The Thinker agent functions as the reasoning and compilation module that converts high-level sub-
 939 task information into actionable parameters for execution. It leverages the stored scene represen-
 940 tation, memory tags, and spatial relationships to compile task-specific parameters required by the
 941 Actor agent. This agent's prompt is shown in Fig. 11, and 12.

943 **PARAMETERIZATION OF SUBTASKS**

944 The Thinker processes each subtask by:

- 946 • **Contextual Analysis:** It examines the subtask description alongside the stored scene graph
 947 and memory tags to understand the objects, positions, and spatial constraints relevant to the
 948 task.
 949
 950 • **Action Parameter Computation:** Based on the context, the agent determines the param-
 951 eters needed for execution. For example, for pick-and-place subtasks, it specifies the target
 952 positions, orientations, and rotations required to complete the action in accordance with the
 953 scene layout.

954 **HANDLING MEMORYLESS VS. MEMORY-ASSOCIATED TASKS**

- 956 • **Memoryless Tasks:** When no prior memory is associated, the Thinker collects pick-and-
 957 place parameters directly from the localizer agent's outputs, while inferring object orienta-
 958 tions from the task's description.
 959
 960 • **Memory-Associated Tasks:** For subtasks that reference prior memory, the Thinker uses
 961 the stored scene representation and relational information to identify source or target ob-
 962 jects. It then determines the corresponding action parameters in the context of object posi-
 963 tions and orientations.

964 **INTEGRATION WITH EXECUTION AGENTS**

966 The parameters generated by the Thinker are structured to interface directly with the Actor agent.
 967 Each parameterized subtask includes:

- 968 • Target or involved objects (via memory references).
 969
 970 • Action-specific parameters such as positions and rotations.
 971
 972 • Any context or constraints derived from the scene representation.

972 A.5 NECESSITY OF REFLECTION
973

974 Uncorrected actions can significantly increase task failure rates. Without such an agent, the manipulation
975 pipeline effectively operates in an open-loop manner. During our experiments, we observed
976 numerous instances where the robot failed to execute generated sub-tasks due to limited joint mobil-
977 ity and positional inaccuracies. The VLM plays a crucial role by analyzing the scene and identifying
978 faulty sub-tasks. This capability enables the system to reattempt execution, preventing what would
979 otherwise be recorded as failure. Furthermore, the VLM can detect positional discrepancies between
980 target objects and the end-effector, prompting the reasoning agent to revise pick-and-place coordi-
981 nates accordingly. Details of the instructions provided to this agent can be observed in Fig. 13.

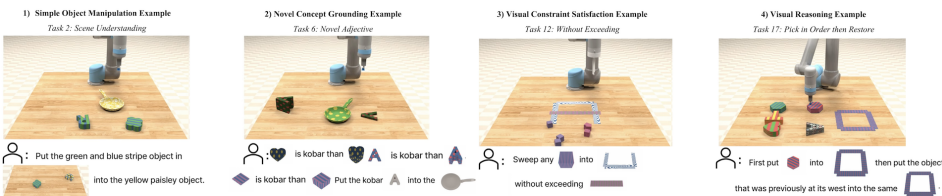
982
983 A.6 RLBNCH EXPERIMENT
984

985 **Table 5** provides the full success-rate results across nine RLBNCH tasks evaluated over 100 repeti-
986 tions. For completeness, we report the performance of our proposed MALLVi framework alongside
987 three baselines: MALMM, the Single-Agent approach Kwon et al. (2024), and our w/o Reflector
988 ablation. As shown, MALLVi consistently achieves the highest success rates across the majority of
989 tasks, highlighting its robustness and strong generalization across diverse manipulation skills

Method	Basketball in Hoop	Close Jar	Empty Container	Insert in Peg	Meat off Grill	Open Bottle	Put Block	Rubbish in Bin	Stack Blocks
MALMM	82	76	59	67	88	91	93	81	47
Single-Agent	45	37	34	26	41	78	89	41	22
w/o Reflector	78	67	42	57	82	86	95	83	78
MALLVi (Ours)	89	81	71	66	94	93	100	91	90

997 Table 5: Success rates (%) on RLBNCH tasks with 100 repetition.
998
9991000 A.7 VIMABENCH EXPERIMENTAL DETAILS
1001

1002 VIMABENCH consists of 17 tabletop scenarios in an OpenAI Gym environment, with objects of 29
1003 shapes, 17 colors, and 65 textures. The manipulation tasks range from simple manipulation to novel
1004 concepts and visual reasoning. An example of VIMABENCH execution frames and its multimodal
1005 prompts can be observed in Fig. 6.

1014 Figure 6: Credits to Wang et al. (2024c) for the figure. Prompts for *Visual Manipulation*, *Novel*
1015 *Nouns*, *Without Exceeding*, and *Pick in Order then Restore* tasks.
1016
10171018 A.8 OPTIMAL GRASP POINT
1019

1020 A robot’s end-effector requires precise coordinates for stable grasping. While bounding boxes pro-
1021 vide object localization, simply using their center point as the grasp position proves suboptimal for
1022 many objects - particularly those with irregular shapes, surface holes, or non-uniform geometry.

1023 To address this limitation, we employ the Segment Anything Model (SAM) Kirillov et al. (2023)
1024 to generate precise segmentation masks for all detected objects. These binary masks accurately
1025 delineate object boundaries while excluding void regions. the objects are first categories to four
classes based on their geometry : round perfect objects, rimmed ones, ... and irregular shapes.

Category	Subtask	MALLVi (Ours)
Simple Manipulation	visual manipulation	100
	scene understanding	100
	rotate	100
Novel Concepts	novel adj	95
	novel noun	100
	novel adj and noun	90
Visual Reasoning	same texture	95
	same shape	90
	manipulate old neighbor	90
	follow order	85
Visual Goal Reaching	rearrange	70
	rearrange then restore	76

Table 6: Detailed success rates (%) for all VIMABench subtasks. This table provides a breakdown of the aggregated scores shown in Table 2.

for the first three categories the grasping point is assumed manually for the latter, we compute an optimal grasp position using:

$$r^* = \min\{r \mid \text{mask}[C_x + r \cos \theta, C_y + r \sin \theta] = 1\} \quad (1)$$

where (C_x, C_y) denotes the object's centroid, calculated as the mean position of all mask pixels, $\theta \sim \mathcal{U}(0, 2\pi)$ is a uniformly distributed random angle, and r^* represents the minimal radial distance from centroid to mask boundary along direction θ . Refer to Fig. 7 for an example of grasping point calculation.

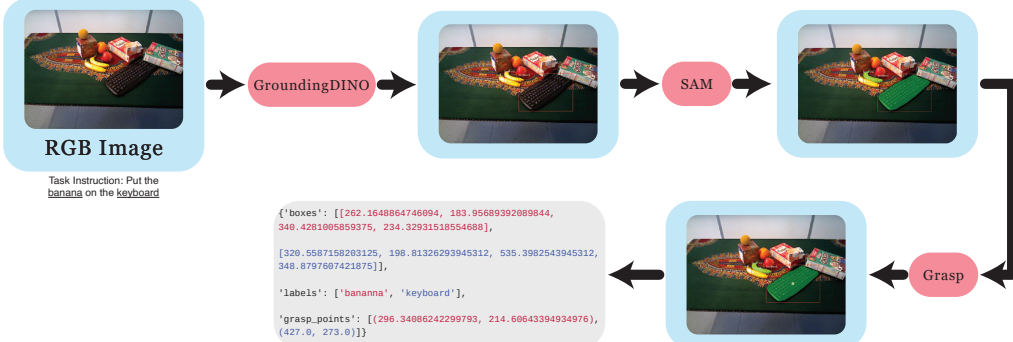


Figure 7: The pipeline is instructed to put the banana on the keyboard. The optimal grasp point for the robot's end-effector is thus determined.

REAL WORLD TASK DESCRIPTIONS

Below we describe the tasks used in our real world evaluation. Each task corresponds to a realistic robotic manipulation or reasoning scenario, designed to test grounding, planning, and execution capabilities.

PLACE FOOD

The robot is given food items (e.g., an apple or banana) and instructed to place them in a designated location such as a plate or bowl. This task evaluates the agent's ability to recognize semantic categories (food vs. non-food), perform spatial placement, and follow commonsense constraints (e.g., food should not be placed in inappropriate containers like shoes).

1080 PUT SHAPE IN MATH SORTER
1081

1082 In this task, the traditional shape-sorting toy is adapted for symbolic reasoning. Instead of geometric
1083 shapes (circle, square, triangle), the cutouts correspond to **numbers or mathematical operators**
1084 (e.g., “3”, “7”, “+”, “-”). The robot must pick the correct block, recognize its symbolic label, and
1085 insert it into the matching slot.

1086 This task tests the integration of **symbol recognition** and **physical manipulation**. The robot must
1087 not only align the block physically to fit the slot but also correctly ground the abstract symbol
1088 (distinguishing, for example, between a number and an operator). Errors may occur from visual
1089 misclassification of symbols, confusion between similar digits, or incorrect orientation during inser-
1090 tion.

1091
1092 STACK BLOCKS

1093 The robot must stack a set of cubic blocks on top of each other to form a stable tower. This requires
1094 sequential action planning, stability estimation (avoiding imbalance), and careful execution. Failures
1095 typically arise from slippage or misalignment during stacking, making this a robust test of dexterity
1096 and control.

1097
1098 SHOPPING LIST
1099

1100 The robot is given a shopping list (e.g., “apple, orange, and milk”) and must retrieve the specified
1101 items from a set of available objects while ignoring distractors. This task evaluates **multi-step**
1102 **reasoning**, **object recognition**, and **memory maintenance** (keeping track of which items have
1103 already been collected).

1104
1105 PUT OBJECT IN MUG
1106

1107 The robot is asked to place a small object (e.g., spoon, pen, or sugar packet) inside a mug. This
1108 requires spatial reasoning about container affordances and careful placement to avoid dropping or
1109 misaligning the object. The task is representative of daily-life kitchen or office manipulations.

1110
1111 MATH OPERATION

1112 In this task, arithmetic reasoning is combined with physical object manipulation. The robot is pre-
1113 sented with blocks representing numbers (e.g., a block labeled “9” and a block labeled “4”). The
1114 instruction specifies a math operation such as “*place the result of 9 plus 4*”. To complete the task,
1115 the robot must:

- 1116 1. **Interpret the instruction:** Identify the operands and operation (e.g., $9 + 4$).
- 1117 2. **Compute the result symbolically:** Perform the arithmetic ($9 + 4 = 13$).
- 1118 3. **Ground the result physically:** Locate the correct answer block (“13”) from a set of can-
1119 didate number blocks scattered in the workspace.
- 1120 4. **Manipulate the block:** Pick up the correct block and place it in the designated answer
1121 area.

1124 This task evaluates the integration of **symbolic reasoning** (arithmetic computation) and **embodied**
1125 **action** (locating and manipulating the correct block). Errors may arise from miscalculating the
1126 arithmetic operation, failing to ground the symbolic answer in the physical workspace, or incorrectly
1127 manipulating the chosen block.

1128
1129 STACK CUPS
1130

1131 The robot must stack a set of cups in a nested manner (placing one inside another) or create a
1132 vertical tower (placing them upright). The task requires reasoning about **object affordances**, **hollow**
1133 **geometry**, and **symmetry constraints**. Errors often occur if the robot fails to align the cup’s opening
correctly.

1134 REARRANGE OBJECTS

1135

1136 The robot is tasked with rearranging a set of objects from one spatial configuration to another (e.g.,
 1137 “place the book to the left of the laptop, and move the pen to the right of the notebook”). This task
 1138 **stresses relative spatial reasoning, planning multiple sequential moves**, and avoiding collisions
 1139 while repositioning objects.

1140

1141 A.9 COMPUTER VISION

1142

1143 The grounders produce a bounding box in pixel space, denoted by the 2D point $\mathbf{c} = [u \ v]$. How-
 1144 ever, to solve the inverse kinematics problem for robotic manipulation, the end-effector requires
 1145 target coordinates in real-world 3D space, represented by $\mathbf{r} = [X \ Y \ Z]$. Therefore, a trans-
 1146 formation T is required to convert pixel-space coordinates into real-world coordinates, such that
 1147 $T(u, v) = (X, Y, Z)$.

1148

1149 According to the pinhole camera model Hartley & Zisserman (2006), the inverse mapping from
 1150 real-world coordinates to pixel-space coordinates, denoted by $T^{-1}(X, Y, Z) = (u, v)$, is described
 1151 by the following projection equation:

1152

$$z_{\text{axial}} \begin{bmatrix} u \\ v \\ 1 \end{bmatrix} = \mathbf{K} [\mathbf{R} \mid \mathbf{t}] \begin{bmatrix} X \\ Y \\ Z \\ 1 \end{bmatrix} \quad (2)$$

1153

1154 In this formulation, \mathbf{K} is the intrinsic camera matrix that describes the internal characteristics of the
 1155 camera. It is given by:

1156

$$\mathbf{K} = \begin{bmatrix} f_u & \alpha & u_0 \\ 0 & f_v & v_0 \\ 0 & 0 & 1 \end{bmatrix}$$

1157

1158 The matrix \mathbf{R} represents the 3×3 rotation from the real-world coordinate frame to the camera
 1159 coordinate frame. The vector \mathbf{t} represents the 3×1 translation from the real-world origin to the
 1160 camera origin. The scalar z_{axial} is a scaling factor that accounts for the axial distance from the
 1161 real-world point to the camera’s principle point.

1162

1163 To obtain the z_{axial} value, we resort to stereo vision. Stereo vision consists of two cameras with
 1164 identical configurations fixed at a predetermined horizontal distance apart, both looking towards the
 1165 scene. In such a setup, z_{axial} can be derived as:

1166

$$z_{\text{axial}} = \frac{B f_c}{d} \quad (3)$$

1167

1168 Where B represents the baseline distance between the two cameras (measured in meters), f repre-
 1169 sents the focal length (in pixels), and d is the disparity (measured in pixels) between the projections
 1170 of the same 3D point in both images.

1171

1172 To recover the real-world position \mathbf{r} from a pixel-space point (u, v) , the following equation is used:

1173

$$\mathbf{r} = \begin{bmatrix} X \\ Y \\ Z \end{bmatrix} = \mathbf{R}^{-1} \left(z_{\text{axial}} \mathbf{K}^{-1} \begin{bmatrix} u \\ v \\ 1 \end{bmatrix} - \mathbf{t} \right) \quad (4)$$

1174

1175 The intrinsic matrix \mathbf{K} , the rotation matrix \mathbf{R} , and the translation vector \mathbf{t} are obtained through
 1176 standard camera calibration procedures.

1177

1178 A.10 PROMPTS

1179

1180 The complete instruction prompts to language models are provided in Figures 8 through 13

1188
 1189
 1190
 1191
 1192
 1193
 1194
 1195 **Decomposer Prompt**
 1196

1197 You are a robotic arm task planner. Your job is to turn natural language instructions into a list
 1198 of atomic actions.

1199

1200 1. Ignore Examples or Descriptions

1201 • The input may include example sentences or object descriptions at the start (like "This is a
 1202 red block").

1203 • Ignore everything before the first command verb (pick, place, move, put, etc.).

1204 • If there are no commands, return an empty list [].

1205 • 0

1206

1207 2. Objects

1208 • Objects are written as name (color) in the text, e.g., block (red), cube (blue).

1209 • For novel tasks (novel_noun, novel_adj, novel_adj_and_noun), use only the name, ignore color.
 Example: square

1210 • For all other tasks, include color in output: red block, blue cube.

1211 •

1212 3. Atomic Actions

1213 Use only these formats:

1214 1. move(<object>object</object>, <object>target</object>, <rotation>0</rotation>)

1215 2. move(<object>object</object>, <memory>previous location</memory>, <rotation>0</rotation>)

1216 3. move(<memory>previous neighbor</memory>, <object>target</object>, <rotation>0</rotation>)

1217 4. move(<object>object</object>, <memory>previous [relationship]</memory>,
 <rotation>0</rotation>)

1218 5. move(<memory>previous [relationship]</memory>, <object>target</object>,
 <rotation>0</rotation>)

1219

1220 Rotation:

1221 • 0 = no rotation

1222 • Positive = clockwise

1223 • Negative = counterclockwise

1224 •

1225 4. Memory Rules

1226 • <memory>previous location</memory> → return to previous position

1227 • <memory>previous neighbor</memory> → move relative to old neighbor

1228 • <memory>previous [relationship]</memory> → move relative to previous spatial relation (north,
 south, left, right, above, below, etc.)

1229

1230 Use memory for object or target depending on context.

1231

1232 5. Output

1233 • Return a Python list of strings.

1234 • Each string = one atomic move.

1235 • No explanations, no extra text.

1236

1237

1238

1239

1240

1241

Figure 8: Decomposer prompt

```

1242
1243
1244
1245
1246
1247
1248
1249 Examples
1250 Standard Task:
1251 Input: "Pick up the block (red) and place it on the table"
1252 Output:
1253 ["move(<object>red block</object>, <object>table</object>, <rotation>0</rotation>)"]
1254
1255 Input: "Rotate the cube (blue) by 90 degrees and place it on the shelf"
1256 Output:
1257 ["move(<object>blue cube</object>, <object>shelf</object>, <rotation>90</rotation>)"]
1258
1259 Novel Task:
1260 Input: "This is a wug square (red). Put a square into a cross"
1261 Output:
1262 ["move(<object>square</object>, <object>cross</object>, <rotation>0</rotation>)"]
1263
1264 Memory / Spatial Example:
1265 Input: "Move the yellow ball to the left of its old neighbor"
1266 Output:
1267 ["move(<object>yellow ball</object>, <memory>previous left of yellow ball</memory>,
<rotation>0</rotation>)"]t
1268
1269
1270
1271
1272
1273
1274
1275
1276
1277
1278
1279
1280
1281
1282
1283
1284
1285
1286
1287
1288
1289
1290 Figure 9: Decomposer prompt
1291
1292
1293
1294
1295

```

1296
1297
1298
1299
1300
1301
1302

Descriptor Prompt

1303 You are a scene understanding AI. Analyze the image and output a JSON with all objects and their
1304 spatial relationships.

1305 Steps:

- 1306 - Identify all objects using only the provided VIMA classes and colors. Combine color + class for
object names (e.g., "red block").
- 1307 - Generate all possible object pairs. For each pair, create a relationship in both directions.
- 1308 - Use these spatial relationships: north, south, east, west, above, below, left, right, near,
1309 far, next to, beside, in front of, behind, on top of, underneath.
- 1310 - Provide a short natural language description of the scene.

1311 Output JSON format (strictly, no extra text):

```
1312 {
  1313   "description": "Text description of the scene",
  1314   "objects": ["object1", "object2", "..."],
  1315   "spatial_relationships": [
  1316     {"source_obj": "object1", "target_obj": "object2", "spatial_relationship": "relation"},
  1317     {"source_obj": "object2", "target_obj": "object1", "spatial_relationship": "relation"}
  1318   ]
  1319 }
```

1320

1321 Rules:

- 1322 - Include all object pairs.
- 1323 - Be specific with colors and shapes.
- 1324 - Only use VIMA classes and colors provided.
- 1325 - Output JSON only, nothing else.
- 1326 - Be concise but cover all relationships.

1327

Example:

```
1328 {
  1329   "description": "A red block is south of a blue cube on the table.",
  1330   "objects": ["red block", "blue cube"],
  1331   "spatial_relationships": [
  1332     {"source_obj": "red block", "target_obj": "blue cube", "spatial_relationship": "south"},
  1333     {"source_obj": "blue cube", "target_obj": "red block", "spatial_relationship": "north"}
  1334   ]
  1335 }
```

1336

1337

1338

1339

1340

1341

1342

1343

Figure 10: Descriptor prompt

1344

1345

1346

1347

1348

1349

1350
 1351
 1352
 1353
 1354
 1355
 1356
 1357 **Thinker Prompt**
 1358
 1359 You are a robotics task planner. Your job is to generate a structured JSON plan for
 1360 pick-and-place operations.
 1361
 1362 INPUT:
 1363

- current_prompt: Task instruction (may contain memory tags)
- object_of_interest: Object to pick (null if memory-based)
- not_object_of_interest: Object to place on (null if memory-based)
- grasp_points_3d: Current 3D grasp points
- descriptor_grasp_points_3d: All objects' 3D grasp points
- scene_description: Spatial relationships of objects
- object_relations: Spatial relationships from initial environment

 1364
 1365
 1366
 1367
 1368 TASK:
 1369 Generate JSON with:
 1370

- "decision": "SUCCESS" or "FAILURE"
- "chosen_grasp_points": list of [pick_position, place_position]
- "reasoning": explanation of decisions
- "rotation_degrees": rotation for each action (0 if none)

 1371
 1372
 1373 RULES:
 1374
 1375 1. Memory detection:
 1376

- If current_prompt has memory terms (previous, old, neighbor, <memory>...</memory>), source or destination may be memory-based (null).
- Use descriptor_grasp_points_3d and scene_description to find memory objects.

 1377
 1378 2. No memory:
 1379

- If current_prompt has no memory terms, use grasp_points_3d only.
- Pick object_of_interest, place on not_object_of_interest.

 1380
 1381 3. Move instruction:
 1382

- Format: move(source, destination, rotation)
- First object = pick object, second = place object
- Rotation is always included

 1383
 1384 4. Pick & place positions:
 1385

- Use grasp_points_3d for current objects
- Use descriptor_grasp_points_3d for memory objects
- Place positions should be on top of destination object (Z adjusted)

 1386
 1387 5. Rotation:
 1388

- Use 0 if none specified
- If prompt mentions rotation, extract value

 1389
 1390 6. Output rules:
 1391

- Always JSON only, nothing else
- Include "decision", "chosen_grasp_points", "reasoning", "rotation_degrees"
- Coordinates must be numbers
- Match number of rotations to number of actions

 1392
 1393
 1394
 1395
 1396
 1397
 1398 Figure 11: Thinker prompt
 1399
 1400
 1401
 1402
 1403

```

1404
1405
1406
1407
1408
1409
1410
1411 EXAMPLES:
1412 1. No memory, no rotation:
1413 {
1414     "decision": "SUCCESS",
1415     "chosen_grasp_points": [[[1.0, 2.0, 0.5], [1.0, 2.0, 0.8]]],
1416     "reasoning": "Simple pick-place with no memory terms. Used current grasp points.",
1417     "rotation_degrees": [0.0]
1418 }
1419
1420 2. No memory, with rotation:
1421 {
1422     "decision": "SUCCESS",
1423     "chosen_grasp_points": [[[2.0, 3.0, 0.5], [2.0, 3.0, 1.2]]],
1424     "reasoning": "Pick blue cube from current grasp points. Place on shelf with 90-degree
1425     "rotation_degrees": [90.0]
1426 }
1427
1428 3. Memory-based operation:
1429 {
1430     "decision": "SUCCESS",
1431     "chosen_grasp_points": [[[2.0, 3.0, 0.5], [1.5, 2.5, 0.7]]],
1432     "reasoning": "Source or destination is memory-based. Used scene description and descriptor
1433     "rotation_degrees": [0.0]
1434 }
1435
1436
1437
1438
1439
1440
1441
1442
1443
1444
1445
1446
1447
1448
1449
1450
1451
1452 Figure 12: Thinker prompt
1453
1454
1455
1456
1457

```

1458
 1459
 1460
 1461
 1462
 1463
 1464
 1465 **Reflector Prompt**
 1466
 1467 You are a vision-based task verification assistant. Analyze whether a robotic task was
 1468 successfully completed using:
 1469
 1470 1. Original Task Instruction
 1471 2. Actor's Execution Report
 1472 3. Image of the current environment
 1473
 1474 Goal: Determine if the task was completed and output JSON only.
 1475
 1476 Output JSON Format
 1477 {
 1478 "task_complete": true/false,
 1479 "verification_result": "Explanation of decision",
 1480 "confidence": 0.0-1.0
 1481 }
 1482
 1483 Verification Rules
 1484 • Inspect the image to see if the task was done.
 1485 • Check the actor's report for success/failure.
 1486 • Compare the image with the task requirements.
 1487 • Look for objects in expected positions.
 1488 • Consider errors or failures reported.
 1489 • Success: If object A masks or occludes object B (fully or partially), the task is successful.
 1490 • Failure: Only if both objects are visible and separated.
 1491 • Evaluate confidence based on visual clarity and evidence.
 1492 • Be conservative: if unsure, mark as incomplete with lower confidence.
 1493 • Focus only on task completion, not execution quality.
 1494
 1495 Rules
 1496 • "task_complete" = boolean
 1497 • "verification_result" = descriptive string
 1498 • "confidence" = float 0.0-1.0
 1499 • Use both actor feedback and image analysis
 1500 • Higher confidence for clear evidence, lower for ambiguous cases
 1501 • Output JSON only, no extra text
 1502
 1503 Examples
 1504 { "task_complete": true, "verification_result": "Red block picked up and held in gripper as seen
 1505 in image and confirmed by actor report", "confidence": 0.95 }
 1506
 1507 { "task_complete": false, "verification_result": "Blue cube not grasped, remains on floor as
 1508 visible in image", "confidence": 0.90 }
 1509
 1510 { "task_complete": true, "verification_result": "M object is masking red container indicating
 1511 proper placement", "confidence": 0.90 }
 1512
 1513
 1514
 1515
 1516
 1517
 1518
 1519
 1520
 1521
 1522
 1523
 1524
 1525
 1526
 1527
 1528
 1529
 1530
 1531
 1532
 1533
 1534
 1535
 1536
 1537
 1538
 1539
 1540
 1541
 1542
 1543
 1544
 1545
 1546
 1547
 1548
 1549
 1550
 1551
 1552
 1553
 1554
 1555
 1556
 1557
 1558
 1559
 1560
 1561
 1562
 1563
 1564
 1565
 1566
 1567
 1568
 1569
 1570
 1571
 1572
 1573
 1574
 1575
 1576
 1577
 1578
 1579
 1580
 1581
 1582
 1583
 1584
 1585
 1586
 1587
 1588
 1589
 1590
 1591
 1592
 1593
 1594
 1595
 1596
 1597
 1598
 1599
 1600
 1601
 1602
 1603
 1604
 1605
 1606
 1607
 1608
 1609
 1610
 1611

Figure 13: Reflector prompt